

# The flow of thin liquid films between rollers

By E. PITTS AND J. GREILLER

Research Laboratories, Kodak Ltd, Wealdstone, Harrow, Middlesex

(Received 7 February 1961)

When rollers, placed horizontally and side by side so that each is half immersed in a tank of liquid, rotate in opposite directions, liquid is carried through the gap between them and divides to form a sheet over each roller. At low speeds the sheets are of uniform thickness across the width of the rollers, but at higher speeds they are regularly ridged owing to alternate increase and decrease in thickness. Preliminary observations led to the development of an approximate theoretical treatment of the even-flow régime and the critical conditions when the ribbed flow is about to begin. Results of this work are in full agreement with detailed experimental results.

---

## 1. Introduction

The production of uniform thin films of liquid as a coating is a frequent industrial requirement, and various methods are used for the purpose. It is a common observation that many of the methods which involve spreading or rolling of the liquid often give rise to very uneven or ribbed layers. It appeared that in spite of the widespread occurrence of the phenomenon, little work had been published relating to it, and no adequate explanation had been given. Accordingly, extensive experimental and theoretical work was carried out in these laboratories on a model consisting of two cylinders placed with their axes parallel and level with the surface of liquid in a tank. Each roller is thus half immersed in liquid. On rotation of the rollers in contrary motion, liquid is drawn up through the narrow gap separating them, and divides to form a sheet over each, returning to the bulk of the liquid. Using this apparatus it has been possible to make many determinations of the position of the meniscus where the liquid divides as a function of the physical and geometrical variables, and to observe the conditions in which the even film of liquid over each roller changes into a regularly rippled sheet. A description of these and other more detailed observations are presented in this paper together with an approximate theoretical treatment of the problem which satisfactorily accounts for all the observed phenomena.

At a late stage in our work we were informed of a similar problem being studied by Dr J. R. A. Pearson, which we discussed with him. The work has recently appeared in an interesting paper (Pearson 1960) in which the spreading of liquid over a plane surface by means of a wedge-shaped spreader is discussed. Pearson was able to account for the appearance of regularly spaced crests and troughs in the emergent thin film running parallel to the direction of motion of the spreader. The observed and calculated periodicities of the ripple were in fair agreement.

His discussion of the problem is, however, in some respects incomplete, since it does not permit the quantitative prediction of the conditions in which the uniform flow, stable for sufficiently low speeds of spreading, changes to the rippled form. Other approximations are made which obscure certain important features of the flow in the region of the meniscus.

We have been able to account for all the main features of the flow in our experiments, together with the quantitative prediction of the critical conditions. The treatment of the problem divides naturally into two parts: the even flow régime before the appearance of ripples, and the critical conditions in which ripples first appear.

## 2. The even flow régime

### 2.1. *Experimental methods*

The arrangement of the rollers in the tank of liquid and their direction of rotation are shown in figure 1. The tank was made of Perspex to allow observations to be made through the sides. Two sizes of roller were used, with known diameters, nominally 1 in. and 2 in. The gap separating the rollers at their closest approach (the nip) could be set from zero to 1 mm with an accuracy and uniformity within

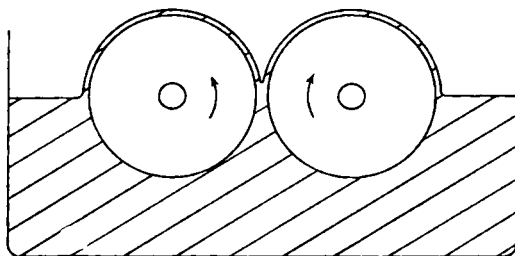


FIGURE 1. Arrangement of rollers in the liquid.

0.015 mm. Because these gaps were so narrow, great care had to be taken in making the rollers to ensure that each was a true cylinder accurately concentric with its spindle. Variation in the width of the gap along its length was about  $\pm 5\%$  in the smallest gaps but much less in the larger gaps. Each roller rotated at the same speed, the maximum rate of rotation being about 75 r.p.m. The viscosity of the liquids used was in the range 0.25–6 poise. During the course of an experiment temperature changes occurred and allowance was made for the consequent change in viscosity when calculating results. When glycerin was used, changes in viscosity also occurred owing to the absorption of moisture from the air. These were known and kept as small as possible.

It became apparent that surface tension could not be changed in a controlled way by using surface-active agents, owing to the rapid rate of expansion of the liquid surface in the region under examination. It was therefore necessary to use liquids having intrinsically different surface tensions.

The basic flow pattern was obtained from photographs taken through the transparent walls of the tank along a direction parallel to the axes of the rollers. Streamlines were made more distinct by the introduction of very small air

bubbles. Other photographs were taken showing the profile of the meniscus at various speeds, together with its position between the rollers. In addition many determinations of meniscus position were made with a travelling microscope.

Sufficiently accurate measurements of the volume of liquid carried through the gap presented great difficulties. The method finally adopted was to collect and weigh the liquid carried by one roller using a tray with a rubber scraper blade. Edge effects were eliminated by using trays of different widths. The scraper could not be made to remove all the liquid from the roller surface and the amount left under different conditions was obtained by absorbing it on filter paper and weighing.

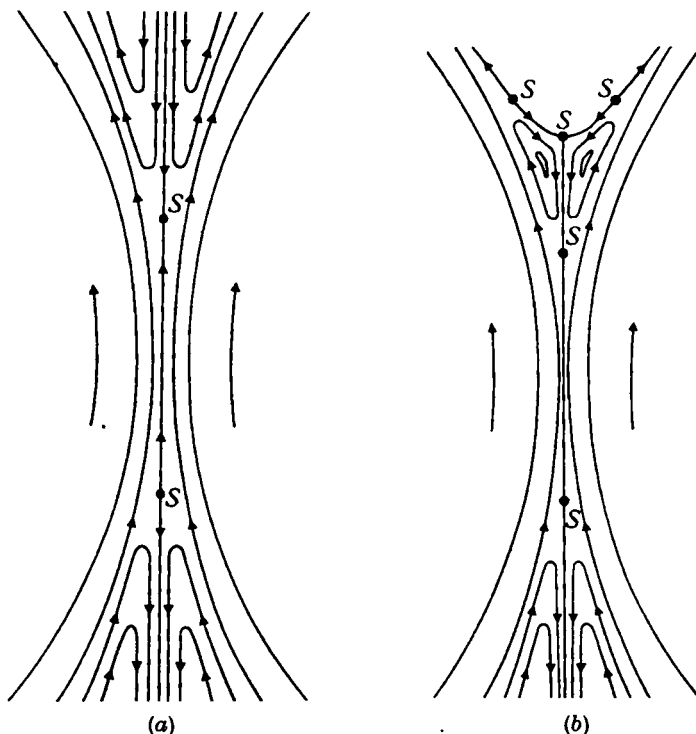


FIGURE 2. (a) Streamlines when rollers are totally immersed. (b) Streamlines when rollers are partially immersed.

### 2.2. Experimental observations

It is of interest to compare the flow pattern when the rollers are completely immersed in the liquid with that when they are half immersed. The streamlines are indicated in figures 2a and b, in which *S* indicates a stagnation point (where the fluid velocity is zero). It will be seen that the flow patterns on the ingoing side are alike, but on the outgoing side the presence of the meniscus causes two areas of circulatory flow, and three extra stagnation points in addition to the centres of the vortices.

By measurement of the many photographs taken, it has been established that, to a very close approximation, the meniscus is parabolic over a large part of its profile.

For a given gap between the rollers the position of the meniscus may be specified by measuring the ratio,  $\sigma_0$ , of the width of the channel at the lowest point of the meniscus to the gap width. In figure 3 the crosses show the value of  $\sigma_0$  for a gap width of 0.020 cm as a function of  $\log(\mu U/T)$ , where  $\mu$  and  $T$  are the viscosity and surface tension of the liquid, and  $U$  is the surface speed of the rollers. Two liquids were used, having surface tensions of 47 and 65 dynes/cm and viscosities were in the range 0.4–5.5 poise. In each experiment the speed was varied by a factor of nearly five, viscosity and surface tension remaining constant. It will be seen that as the speed is increased,  $\sigma_0$  decreases, i.e. the meniscus moves in towards the nip. Similar results are found for other gap widths.

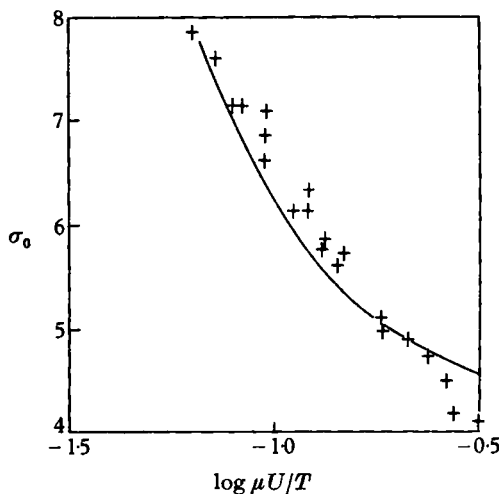


FIGURE 3. The position of the meniscus: + experimental observations; - theoretical curve.

Elementary considerations suggest that if  $2h$  is the width of the nip, the quantity of liquid carried through per second per unit length of the roller will be  $2\lambda U h$ , where  $\lambda$  is a number of order of magnitude unity. As has already been mentioned, the experimental measurement of the quantity carried through, and hence the determination of  $\lambda$  in given flow conditions, was difficult to achieve with sufficient accuracy. Liquid escaped collection, and the accuracy with which the smallest gaps could be set was probably not better than  $\pm 10\%$ . For a range of flow conditions the mean of the observed values of  $\lambda$  was 1.33, individual readings ranging from 1.38 to 1.26. A slight decrease in  $\lambda$  with increasing speed is indicated by the results.

In the next section we shall give an approximate theoretical account of this type of flow, and in §2.4 compare theory with the experimental results just described.

### 2.3. Theory

The flow pattern in the region of the meniscus, as revealed by experiment, is complicated and an exact theoretical treatment of the problem appears extremely difficult. Accordingly, we shall present a treatment which although approximate,

nevertheless reveals the most important of the relationships and accounts for the main experimental results.

The motion of the liquid in the region where the channel is narrow is predominantly determined by the drag due to the moving rollers and the variation in the width of the channel. It may be shown that inertia terms in the hydrodynamic equations can be neglected without serious error. Terms representing the effect of gravity were included in the original treatment but are here omitted for simplicity, since their influence is small except at the lowest speeds of rotation and for the largest gap widths. Pearson has outlined in his paper the arguments justifying these approximations.

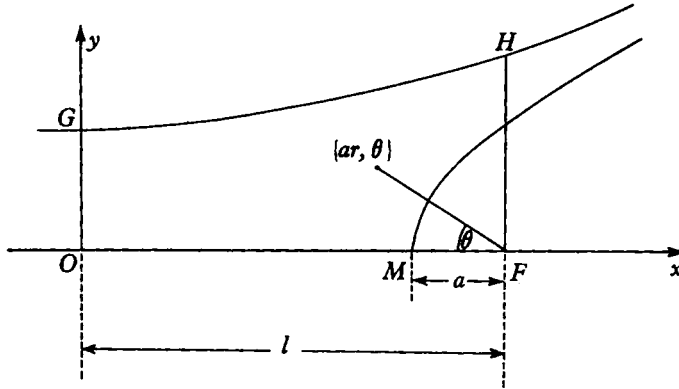


FIGURE 4. Co-ordinate system used to describe flow in the vicinity of the meniscus.

In principle, it should be possible to deduce both the form and the position of the free liquid surface from purely theoretical considerations. This degree of generality will not be attempted here. Instead, we shall make use of the experimental observations that the meniscus has a parabolic profile, and find theoretically its size and position along the axis of symmetry.

First, we shall ignore the presence of the meniscus and calculate the flow in the narrow part of the channel. It will be convenient to use the co-ordinate system shown in figure 4. The  $x$ -axis is along the axis of symmetry, the  $y$ -axis is in the plane through the axes of the rollers which are parallel to the  $z$ -axis. There is no component of fluid velocity in the  $z$ -direction. Let  $OG$  equal  $h$  (half the gap width) and let the radius of the rollers be  $R$ . A brief preliminary investigation suggests that new variables  $\xi$  and  $\eta$ , defined by the equations

$$x = \xi(Rh)^{\frac{1}{2}}, \quad y = \eta h \tag{2.1}$$

are suited to this problem. We can then use the ratio

$$\delta = h/R \tag{2.2}$$

as a small parameter (of the order  $5 \times 10^{-3}$ ) in the development of the solution. If the surface of the roller is defined by the equation

$$\eta = \sigma(\xi), \tag{2.3}$$

elementary geometry shows that

$$\sigma = 1 + \frac{1}{2}\xi^2 + O(\delta). \tag{2.4}$$

If the component of velocity in the  $x$ -direction is written  $Uu$ , that in the  $y$ -direction  $\delta^{\frac{1}{2}}Uv$ , where  $U$  is the velocity of the surface of the roller, and

$$P = p h^{\frac{1}{2}} / \mu U R^{\frac{1}{2}}, \quad (2.5)$$

where  $p$  is the pressure and  $\mu$  the viscosity of the liquid, the hydrodynamic equations become (neglecting inertia terms and the force due to gravity)

$$\frac{\partial P}{\partial \xi} = \frac{\partial^2 u}{\partial \eta^2} + O(\delta), \quad (2.6)$$

$$\frac{\partial P}{\partial \eta} = O(\delta). \quad (2.7)$$

The continuity equation is

$$\frac{\partial u}{\partial \xi} + \frac{\partial v}{\partial \eta} = 0. \quad (2.8)$$

At the roller surface the liquid velocity must equal that of the roller. Hence when  $\eta = \sigma$

$$u = 1 + O(\delta). \quad (2.9)$$

Also the quantity of liquid per second per unit length crossing a plane perpendicular to the  $x$ -axis and extending to the surfaces of the rollers must be constant. If this quantity is  $2\lambda U h$ , then we must have

$$\lambda = \int_0^\sigma u d\eta. \quad (2.10)$$

If we neglect terms  $O(\delta)$  we find that

$$u = 1 + \frac{3}{2}(\sigma - \lambda)(\eta^2 - \sigma^2)/\sigma^3 \quad (2.11)$$

and

$$P = 3 \int^\xi \left( \frac{\sigma - \lambda}{\sigma^3} \right) d\xi. \quad (2.12)$$

We notice that the position of the stagnation point on the axis is given by

$$\sigma = 3\lambda. \quad (2.13)$$

Equivalent results have also been given by other workers (for example, Banks & Mill 1954 and Hopkins 1957). If the rollers are completely immersed, it is easily shown that  $\lambda$  must be  $\frac{4}{3}$ , to this degree of approximation.

We shall now attempt to describe conditions in the neighbourhood of the meniscus by adding to the above solution terms which are important only near the meniscus, and which decrease rapidly elsewhere.

It is convenient to use cylindrical co-ordinates centred on the focus  $F$  of the parabolic meniscus, whose latus rectum is  $4a$  (see figure 4). The distance from the nip to the focus is  $l$ . (Both  $l$  and  $a$  will be evaluated theoretically.) The radius vector has length  $ar$ , where  $r$  is dimensionless. If we introduce a stream function  $\psi$ , such that the component velocities divided by  $U$  are respectively

$$v_r = -\frac{1}{r} \frac{\partial \psi}{\partial \theta}, \quad v_\theta = \frac{\partial \psi}{\partial r}, \quad (2.14)$$

the Stokes equations are

$$\frac{a}{\mu U} \frac{\partial p}{\partial r} = -\frac{1}{r} \frac{\partial}{\partial \theta} \nabla^2 \psi, \quad \frac{a}{\mu U} \frac{1}{r} \frac{\partial p}{\partial \theta} = \frac{\partial}{\partial r} \nabla^2 \psi, \quad (2.15)$$

and  $\psi$  must satisfy the relation

$$\nabla^4 \psi = 0. \quad (2.16)$$

The equation of the parabolic surface of the meniscus is

$$r(1 + \cos \theta) = 2. \quad (2.17)$$

The boundary conditions are as follows. The velocity normal to this surface must be zero, i.e., on the surface,  $\psi$  is a constant, which may be put equal to zero

$$\psi = 0. \quad (2.18)$$

Also, the tangential stress in the liquid must be zero on the surface. If  $\sigma_r$ ,  $\sigma_\theta$  and  $\tau_{r\theta}$  are the stresses defined in the usual way for cylindrical co-ordinates, and  $\phi$  is the angle between the tangent to the surface at a point and the normal to the radius vector at the point, then the vanishing of the tangential stress may be written

$$(\sigma_r - \sigma_\theta) \sin \phi \cos \phi + \tau_{r\theta} (\cos^2 \phi - \sin^2 \phi) = 0. \quad (2.19)$$

From the equation for the parabola, it follows that

$$\phi = \frac{1}{2}\theta, \quad (2.20)$$

and, from this relation and the definitions of the stresses, the condition for zero tangential stress becomes

$$2 \frac{\partial v_r}{\partial r} \sin \theta + \left( \frac{\partial v_\theta}{\partial r} - \frac{v_\theta}{r} + \frac{1}{r} \frac{\partial v_r}{\partial \theta} \right) \cos \theta = 0. \quad (2.21)$$

The outward normal component of stress  $S_N$  is given by

$$S_N = \sigma_r \cos^2 \phi + \sigma_\theta \sin^2 \phi - 2\tau_{r\theta} \sin \phi \cos \phi. \quad (2.22)$$

Using the above definitions together with the condition (2.19), we find

$$S_N = -p + \frac{2\mu U}{a \cos \theta} \frac{\partial v_r}{\partial r}. \quad (2.23)$$

$S_N$  must equal the normal stress on the surface due to atmospheric pressure and the effect of surface tension  $T$ . When the radius of curvature at a point on the surface is calculated, and measuring pressure in excess of atmospheric pressure, the condition expressing continuity of normal stress becomes

$$\frac{T}{\mu U} \frac{(1 + \cos \theta)^{\frac{3}{2}}}{2^{\frac{3}{2}}} = -\frac{ap}{\mu U} + \frac{2}{\cos \theta} \frac{\partial v_r}{\partial r}. \quad (2.24)$$

In addition, the resultant velocity at the surface of the rollers must equal  $U$ , and to ensure the constancy of net flux,  $\psi$  must be constant there.

We shall suppose that the solution of equation (2.16) relevant to this problem may be written

$$\psi = \sum_1^\infty \sin m\theta (A_m r^m + C_m r^{m+2} + B_m r^{-m} + D_m r^{2-m}), \quad (2.25)$$

where the coefficients  $A_m$  and  $C_m$  are those corresponding to the solution (2.11). The remaining terms express the influence of the meniscus. The pressure is then given by

$$p = -4\mu \sum_1^{\infty} \cos m\theta [(m+1)C_m r^m + (m-1)D_m r^{-m}] + c, \quad (2.26)$$

where  $c$  is a constant, and equation (2.21) gives

$$0 = \sum_1^{\infty} \sin(m+1)\theta [m(m+1)B_m r^{-m-2} + m(m-1)D_m r^{-m}] \\ + \sum_1^{\infty} \sin(m-1)\theta [m(m-1)A_m r^{m-2} + m(m+1)C_m r^m], \quad (2.27)$$

where  $r$  is defined by equation (2.17).

If  $\sigma_1$  is the ratio of the lengths  $FH$  to  $OG$ , by straightforward methods we find the following expressions for the  $A$  and  $C$  coefficients:

$$\left. \begin{aligned} A_1 &= \frac{1}{2}(3\kappa - 1), & C_1 &= \frac{3}{2}\alpha(1 - \kappa), \\ A_2 &= \frac{3}{2}\kappa\beta, & C_2 &= \frac{1}{2}\alpha\beta(1 - \frac{3}{2}\kappa), \\ A_3 &= -\frac{1}{2}C_1, & C_3 &= 0, \\ A_4 &= -\frac{1}{2}C_2, & C_4 &= 0, \end{aligned} \right\} \quad (2.28)$$

where we have defined

$$\left. \begin{aligned} \kappa &= \lambda/\sigma_1, & \beta &= la/\sigma_1 Rh, \\ \alpha &= (a/\sigma_1 h)^2, & \sigma &= \sigma_1(1 - \beta r \cos \theta) + O(\delta), \end{aligned} \right\} \quad (2.29)$$

and neglected all terms  $O(\beta^2)$  and  $O(\delta)$ . (Development of the theory confirms the experimental result that in cases of interest  $\beta$  is less than 0.09.)

We have now to determine the  $B$  and  $D$  coefficients so that the boundary conditions are satisfied. This problem is made particularly difficult by the complicated geometry of the surfaces in the neighbourhood of the meniscus. Instead of attempting to satisfy conditions exactly at both boundaries we shall take three terms which decrease as  $r$  increases, and choose the coefficients so that over the meniscus the boundary conditions are satisfied for terms of order  $\theta$  and  $\theta^3$  in the expansion of equations (2.18), (2.21) and (2.24). Since  $D_1$  may without loss of generality be assumed to be zero, we have retained  $B_1$ ,  $D_2$  and  $D_3$ , i.e. terms in the velocities of order  $r^{-1}$  and  $r^{-2}$ . The outcome of other choices has been investigated, and it appears that the general result is not greatly affected. In making this approximation the boundary conditions at the surface of the roller are violated. However, very interesting and useful results can be obtained in spite of this defect.

Equations (2.18), (2.21) and (2.24) each give two equations corresponding to the coefficients of  $\theta$  and  $\theta^3$ . These six equations may be solved and after lengthy algebra give  $A_1$ ,  $C_1$ ,  $B_1$ ,  $D_2$  and  $D_3$  in terms of  $T/\mu U$ ,  $A_2$ , and  $C_2$ . Finally, there is an expression which in effect relates  $p$  and  $T/\mu U$ ,  $A_2$  and  $C_2$ . The expressions for  $A_1$ ,  $C_1$  and that involving  $p$  may be written after some rearrangement

$$3\kappa = 1 - T/29.3\mu U - 2.44\kappa\beta + 3.28\alpha\beta(1 - \frac{3}{2}\kappa), \quad (2.30)$$

$$\alpha = (T/56.4\mu U + 0.59\kappa\beta)/[1 - \kappa + 3.20\beta(1 - \frac{3}{2}\kappa)] \quad (2.31)$$



and  $\sigma_1 q(\sigma_1, \lambda) = (2h/\alpha R)^{\frac{1}{2}} [0.148T/\mu U + 0.30\kappa\beta + 1.65\alpha\beta(1 - \frac{3}{2}\kappa)],$  (2.32)

where  $q(\sigma_1, \lambda) = -2 \int_{-\infty}^{\xi_0} \left( \frac{\sigma - \lambda}{\sigma^3} \right) d\xi$  (2.33)

and  $1 + \frac{1}{2}\xi_0^2 = \sigma_1(1 - \beta).$  (2.34)

Use of the relation (2.4) in evaluating the infinite integral in (2.33) introduces only negligible error.

From these equations we wish to find  $\kappa$ ,  $\alpha$  and  $\lambda$  for a given value of  $T/\mu U$ . It will be seen that the expression for  $\kappa$  involves  $\kappa$  on the right-hand side, but since these terms are small a first approximation to  $\kappa$  is immediately obtained. Using this and assuming  $\lambda$  to be  $\frac{4}{3}$ , a rough value of  $\sigma_1$  is obtained. From equation (2.31),

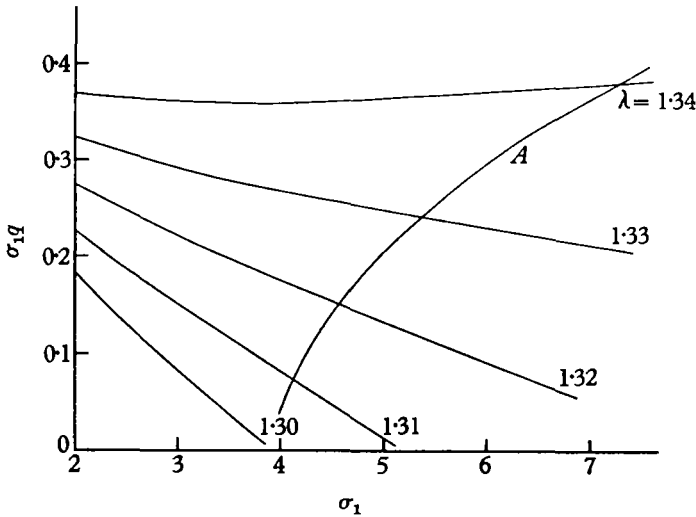


FIGURE 5. Values of  $\sigma_1 q$  as a function of  $\sigma_1$  and the appropriate value of  $\lambda$ .

by ignoring terms involving  $\beta$ , we next obtain a rough value of  $\alpha$ . From our knowledge of  $\sigma_1$  we can derive a rough value for  $l$  by geometry, and hence find  $\beta$  approximately. This enables a new derivation of  $\kappa$  to be made from equation (2.30). The process can be repeated to obtain better approximations. When these are obtained, we can calculate the right-hand side of equation (2.32). The left-hand side of this equation is independent of  $T/\mu U$ , and may be calculated as a function of  $\sigma_1$ ,  $\lambda$  and  $\beta$ . These values are shown in figure 5. Since we know the value of the right-hand side of equation (2.32), i.e. the numerical value of  $\sigma_1 q$ , and also the value of  $\sigma_1$  we can therefore obtain a new value of  $\lambda$ . This can then be used to improve the values of  $\kappa$  and  $\alpha$ .

From curve A of figure 5 we can find how the value of  $\lambda$  changes as  $\sigma_1$  changes (due to changes in  $T/\mu U$ ). These calculations also enable us to find the value of  $\sigma_0$  corresponding to the cross-section at M.

#### 2.4. Comparison with experiment

From these results the value of  $\sigma_0$  as a function of  $\log(\mu U/T)$  is known and has been indicated by the smooth curve in figure 3. It will be seen that the extent of the agreement is very satisfactory.

Similar agreement is found for other gap widths. The region where the discrepancy is largest is at small values of  $\sigma_0$ , i.e. high speeds of rotation. This may perhaps be because at low speeds the roller surfaces (where boundary conditions are violated) are relatively more distant from the region of the meniscus near the axis of symmetry, than when the speed is large. We might then expect that incorrect boundary conditions at the rollers would have most effect at high speeds.

Reference to figure 5 shows that as  $\sigma_1$  decreases,  $\lambda$  also decreases. The substantiation of this theoretical change from about 1.34 when  $\sigma_1 = 7$ , to 1.30 when  $\sigma_1 = 4$  would require experimental accuracy which could not be achieved without completely redesigning the apparatus. Nevertheless, the predicted change is in the same direction as the experimental trend.

### 3. Critical conditions

#### 3.1. Experimental observations

As has already been described in §2.2, an increase in speed of rotation of the rollers causes the meniscus to recede towards the nip. When the meniscus is close to the stagnation point  $S_0$  (see figure 2*b*), the circulatory regions are too small to be seen clearly. Any further increase in speed causes a change to take place in the flow pattern. In the region of the meniscus the velocity now has a component parallel to the axes of the rollers. The previously smooth sheet of liquid over each roller becomes regularly rippled across its width, with a consequent regular disturbance of the evenness of the liquid sheets. When first clearly visible, this ripple is of low wave-number (3 or 4 crests/in.) and is constant across the whole width of the rollers. With all conditions fixed, the surface remains steady, the cross-section of each line being of the same form and wavelength. The crests on one roller are directly opposite those on the other. A schematic diagram of the appearance of the liquid is shown in figure 6.

A further steady increase in speed results at first in an increase in amplitude only, then, after a slight wandering and merging of the lines, in an increase in their wave-number. This new state is again stable over a range of speeds, only changing in amplitude. Another transition follows and this cycle is repeated until eventually the ripples are very numerous (about 25/in.).

It is of interest to measure conditions under which the ripple first appears. This has been done for varying speed, viscosity and gap width, and with different liquids to investigate the effect of surface tension. It is difficult to judge when ripples of very small amplitude are first present, and so, to obtain more consistent results, a criterion was chosen in which the ripples were of sufficient amplitude to be unmistakable.

The results of these observations are shown in figure 7. The product  $\mu UR$  is shown as a function of  $Th$  in conditions under which ripples first appear. The

values of viscosity range between 0.4 and 5.4 poise and the gap varies between 0.005 cm (0.002 in.) and 0.05 cm (0.02 in.). Two sets of rollers were used, with radii nominally of 0.5 and 1 in. Two liquids were used, a glycerin-water mixture

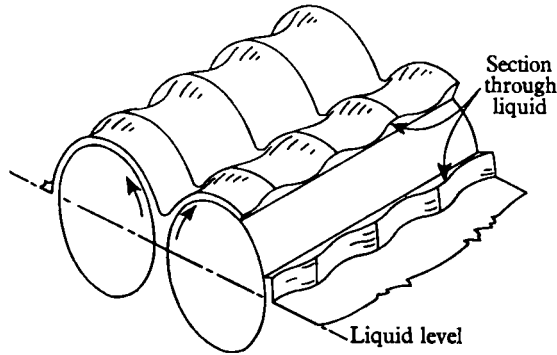


FIGURE 6. The appearance of ripples (not drawn to scale).

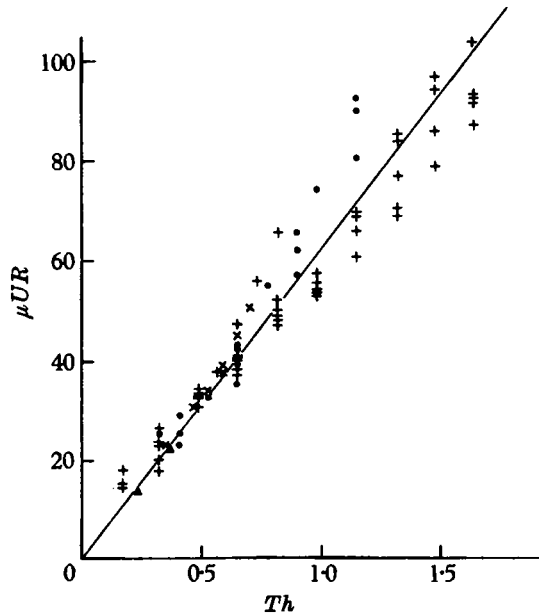


FIGURE 7. Critical conditions as determined by experiment. + Glycerin, 2 in. roller. ● Glycerin, 1 in. roller. × Lactic acid, 2 in. roller. ▲ Lactic acid, 1 in. roller.

with a surface tension of 65, and pure lactic acid with a surface tension of 47. It will be seen from the figure that when conditions are critical and ripples are first recognisably present  $\mu UR/Th \simeq 62$ . In §3.3 we shall discuss the reliability of this result more fully. Having regard to the experimental difficulties, especially the difficulty of deciding on the presence or absence of a ripple, the scatter of the experimental results is not excessive.

From this result it will be seen that the smaller the surface tension of the liquid or the smaller the gap, the lower the velocity at which ribbing occurs. Increasing

the viscosity of the liquid or the radius of the rollers likewise causes ribbing to appear at lower velocities. The effect of surface tension may be strikingly demonstrated by allowing ether vapour to collect near the meniscus when ripples are absent. Adsorption of ether causes a large reduction in surface tension which is usually sufficient to give rise to the appearance of ripples, because (at fixed speed) the critical value of the above ratio has been exceeded.

### 3.2. Theory

The experimental results just described demonstrate the importance of the dimensionless ratio  $\mu UR/Th$  in determining the flow conditions. Before giving a detailed theoretical explanation, it will be helpful to give an outline of the main physical considerations to show qualitatively how this result arises.

Owing to the curvature of the meniscus, there is a drop in pressure on crossing the boundary equal to  $T/2a$ . The gradient of the pressure (equation (2.12)) near the meniscus is given approximately by the equation

$$dp/dx = 3\mu U(\sigma - \lambda)/\sigma^3 h^2.$$

Now imagine that at two different positions across the width of the roller, owing to a small perturbation, the menisci cut the axis at different distances  $x$  and  $x + dx$  from the nip. At the meniscus farthest from the nip, the pressure drop will be less than that at the other site because  $a$  has increased. The pressure drop behind this meniscus but at a distance  $x$  from the nip will therefore be

$$\frac{T}{2a} + \left[ \frac{d}{dx} \left( \frac{T}{2a} \right) + \frac{dp}{dx} \right] dx.$$

Thus, compared with the pressure at the other meniscus, there is a pressure difference of

$$\left( -\frac{T}{2a^2} \frac{da}{dx} + \frac{dp}{dx} \right) dx$$

tending to produce sideways motion of the liquid. If this difference is positive, there will be a tendency for liquid to flow towards the point where the meniscus is farther out, so that the perturbation may be increased, and hence instability arise. We might therefore expect our stability criterion to be

$$\frac{dp}{dx} < \frac{T}{2a^2} \frac{da}{dx}.$$

From equation (2.31) it will be seen that we may write  $\alpha = kT/\mu U$ . The quantity  $k$  is approximately constant in the conditions of interest. Assuming  $k$  is strictly constant, we may evaluate  $da/dx$  using (2.29), and the above criterion for instability becomes

$$\frac{3(\sigma - \lambda)}{\sigma} < \left( \frac{Th}{\mu UR} \right)^{\frac{1}{2}} \left( \frac{\sigma - 1}{2k} \right)^{\frac{1}{2}}$$

after cancellation of common factors. This result shows that  $\mu UR/Th$  depends on  $\sigma$  and since this quantity only varies slowly with  $T/\mu U$ , we have an indication that, at least approximately,  $\mu UR/Th$  is a constant when conditions are critical. Evaluation of the constants gives the result that, when conditions are critical,

$\mu UR/Th$  has a value about 10, which is the order of magnitude of the experimental result. This suggests that the above argument is a sound basis for a more thorough analysis.

It will be seen that a vital step in this argument is the use of equation (2.31). The plausible hypothesis that the radius of curvature of the surface may approximately be put simply proportional to the channel width alone leads by a similar argument to the appearance of the group  $\mu UR^{\frac{1}{2}}/Th^{\frac{1}{2}}$ , which is not in accord with experiment. This assumption was however used successfully by Pearson (1960) in his discussion of another problem, but it evidently cannot be used here.

Two important factors have been entirely omitted in the above, viz. the effect of curvature of the meniscus in the other plane, and the variation in the amount of liquid carried away as a function of meniscus position. In the following we shall consider these additional factors.

It will be convenient to follow the analysis and notation used by Pearson, making use of equation (2.31) at a later stage, so that comparison with Pearson's work is easier. We need to know the effect of small changes in the shape of the meniscus on the flow pattern. Using the Cartesian co-ordinate system shown in figure 4, we shall suppose that the meniscus cuts the  $(x, z)$ -plane in the curve

$$x = x_0 + \epsilon \cos nz, \quad (3.1)$$

where  $\epsilon$  is a small length whose square can be neglected. Since the meniscus cuts the  $(x, y)$ -plane in a parabola (latus rectum  $4a$ ) the expression for the pressure reduction due to surface tension is found from the sum of the principal curvatures of the surface, and is

$$T \left( \frac{1}{2a} - \epsilon n^2 \cos nz \right). \quad (3.2)$$

We may find  $\partial p/\partial z$  by the same argument as that used earlier, but using the expression (3.2) for the pressure drop. After a little manipulation, we find that

$$\frac{\partial p}{\partial z} = \epsilon n \left[ \frac{3\mu U(\sigma_0 - \lambda)}{h^2 \sigma_0^3} - T \left( \frac{1}{2a^2} \frac{da}{dx} + n^2 \right) \right] \sin nz. \quad (3.3)$$

The effect of this small pressure on the flow pattern may be found by conventional perturbation methods. Suppose that the velocities of the liquid in the  $x$ - and  $z$ -directions are increased by the quantities  $u'$  and  $w'$ , where

$$\frac{u'}{U} = \epsilon F(x) \left( \frac{\eta^2}{\sigma^2} - 1 \right) \cos nz, \quad (3.4)$$

$$\frac{w'}{U} = \epsilon G(x) \left( \frac{\eta^2}{\sigma^2} - 1 \right) \sin nz. \quad (3.5)$$

Both these additional velocities vanish at the surfaces of the rollers. If  $p'$  is the perturbation of the pressure, the perturbed parts of the equations of motion are approximately

$$\frac{\partial p'}{\partial x} = \frac{\mu}{h^2} \frac{\partial^2 u'}{\partial \eta^2}, \quad (3.6)$$

$$\frac{\partial p'}{\partial z} = \frac{\mu}{h^2} \frac{\partial^2 w'}{\partial \eta^2}. \quad (3.7)$$

The continuity of cross-sectional flow implies that

$$\frac{\partial}{\partial x} \int_0^\sigma u' d\eta + \frac{\partial}{\partial z} \int_0^\sigma w' d\eta = 0. \quad (3.8)$$

By differentiating equations (3.6) and (3.7) and eliminating  $p'$ , we find after substitution that

$$\frac{d}{dx} \left( \frac{G}{\sigma^2} \right) + \frac{nF}{\sigma^2} = 0, \quad (3.9)$$

and from equation (3.8)

$$\frac{d}{dx} (\sigma F) + n\sigma G = 0. \quad (3.10)$$

Eliminating  $F$  from these equations gives

$$G'' - \frac{\sigma' G'}{\sigma} - \left( n^2 + \frac{2\sigma''}{\sigma} \right) G = 0, \quad (3.11)$$

where primes denote differentiation with respect to  $x$  (cf. Pearson).

From equations (3.7) and (3.3) we find that

$$\frac{3}{\sigma_0^2} \left( 1 - \frac{\lambda}{\sigma_0} \right) - \frac{h^2 T}{\mu U} \left( \frac{a'}{2a^2} + n^2 \right) = \frac{2G_0}{n\sigma_0^2}, \quad (3.12)$$

where  $G_0$  is the value of  $G(l-a)$ . If we write

$$\alpha = kT/\mu U \quad (3.13)$$

then  $k$  is defined by equation (2.31) and varies only very slowly with  $T/\mu U$ . Using equation (3.13) and the definition of  $\sigma_1$  (equation (2.4)) to find  $a'$ , equation (3.12) may be written

$$\frac{3}{\sigma_0^2} \left( 1 - \frac{\lambda}{\sigma_0} \right) - \left( \frac{\sigma_1 - 1}{2k} \right)^{\frac{1}{2}} / \sigma_1^2 \Theta - N \Theta^{-2} = \frac{2G_0}{n\sigma_0^2}, \quad (3.14)$$

where

$$\Theta = (\mu UR/Th)^{\frac{1}{2}}, \quad N = Rhn^2, \quad (3.15)$$

and  $\sigma_1 h$  and  $\sigma_0 h$  are half the width of the channel at the focus and nose of the meniscus, respectively. It will be noted that  $\Theta$  is the parameter whose value was found from experiment to be constant when conditions are critical.

The amount of liquid flowing in the  $x$ -direction due to the perturbation is

$$h \int_0^\sigma u' d\eta = -\frac{2}{3} U h \sigma F \epsilon \cos nz. \quad (3.16)$$

If the system were in equilibrium, the change in  $\lambda$  corresponding to the changed position of the meniscus would be  $\epsilon \cos nz d\lambda/dx$  so that the amount of liquid removed would be increased by an amount  $U h \epsilon \cos nz d\lambda/dx$ . If the latter is less than the expression (3.16) we should expect the perturbation to be increased. Hence the condition for instability is

$$d\lambda/dx < -\frac{2}{3} \sigma F. \quad (3.17)$$

Replacing  $F$  in terms of  $G$ , the condition may be written

$$\frac{d\lambda}{dx} < -\frac{2\sigma}{3n} \left( G'_0 - \frac{2\sigma'}{\sigma} G_0 \right). \quad (3.18)$$

To obtain numerical results, we must solve equation (3.11), using the condition (3.14), and substitute for  $G_0$  in the inequality (3.18). The value of  $d\lambda/dx$  may be

derived from the graph shown in figure 5. The outline of this work is indicated in the Appendix. The final result is

$$4 \cdot 24(1 + \beta)^4 \frac{(\sigma_0 - 1)^{\frac{1}{2}}}{\sigma_1} \frac{d\lambda}{d\sigma_1} < \left[ 3 \left( \frac{\sigma_1}{\sigma_0} \right)^2 \left( 1 - \frac{\lambda}{\sigma_0} \right) - \left( \frac{\sigma_1 - 1}{2k} \right)^{\frac{1}{2}} \Theta^{-1} - \sigma_1^2 \Theta^{-2} N \right] \left[ \rho - \frac{3(\sigma_0 - 1)^{\frac{1}{2}}}{2^{\frac{1}{2}} \sigma_0} \right], \quad (3.19)$$

where 
$$\rho^2 = N + 3 \left( \frac{1}{\sigma_0} - \frac{1}{2\sigma_0^2} \right). \quad (3.20)$$

For convenience in the discussion of the condition for instability we write (3.19) in the form  $(A) < (B)(C)$ .

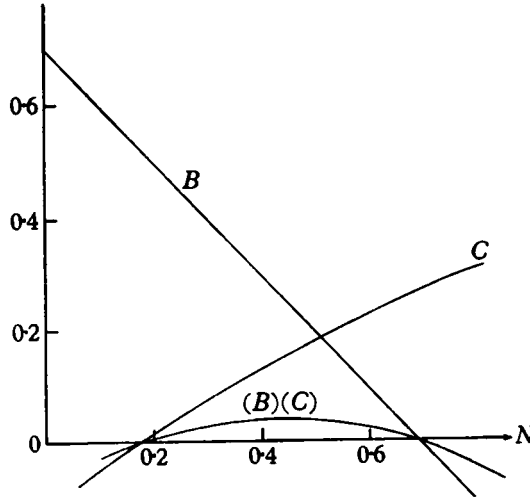


FIGURE 8. Values of the terms  $(B)$ ,  $(C)$ , and  $(B)(C)$  as functions of  $N$ .

### 3.3. Comparison with experiment

Numerical results are obtained from equation (3.19) in the following way. For a given value of  $\Theta$  we may find the values of  $\sigma_1$  and  $\sigma_0$  and hence the value of  $(A)$ . The value of  $(B)$  is a function which decreases linearly with increasing  $N$ , a measure of the ripple wave-number. The quantity  $(C)$  increases as  $N$  increases. In figure 8 values of  $(B)$ ,  $(C)$  and the product  $(B)(C)$  are shown as functions of  $N$ , for the case  $T/\mu U = 8$  and  $h/R = 0.004$ . For given  $\Theta$  as  $N$  varies there is a particular value of  $N$  which makes  $(B)(C)$  a maximum. We must find the value of  $\Theta$  such that the maximum value of the product just equals  $(A)$ .

The results of these calculations are shown in figure 9, where curve  $M$  shows the maximum value of  $(B)(C)$  and curve  $A$  the value of  $(A)$ . For values of  $\Theta$  less than 5.3 the maxima are all less than  $(A)$ , i.e. conditions are always stable. For values of  $\Theta$  greater than 5.3, conditions are unstable, i.e. for  $(\mu UR/Th)$  greater than 28. The experimental value for this ratio is 62, which is known to be too high owing to difficulties in detecting the onset of ribbing (see next section).

The value of  $n$  at the critical point is 3.48, which means that the distance between ridges is 1.8 cm. Experimental observations showed that across the

5 in. roller there were approximately 17 crests, so that the observed distance was 0.75 cm.

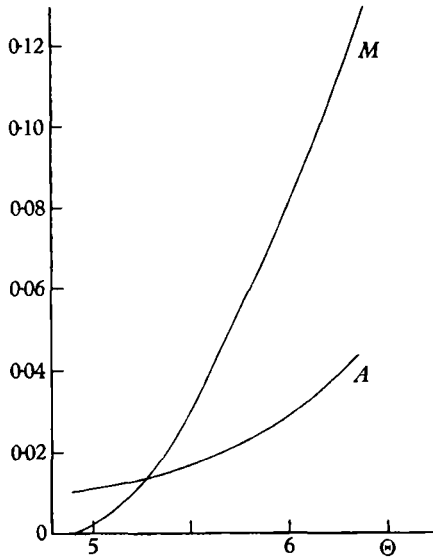


FIGURE 9. Theoretical determination of the critical value of  $\Theta$ .

#### 4. Discussion

The general agreement between theory and experiment for the even flow régime and also for the critical conditions at the transition shows that all the most important features have been satisfactorily explained. In view of the complexity of the problem and the approximations in the theoretical treatment the extent of the numerical agreement is also very satisfactory. A closer examination of the comparison between theory and experiment will show in more detail the extent of the agreement and what shortcomings still remain.

Reference to figure 3 shows that the theory is moderately successful in predicting the position of the meniscus, but the curvature of the theoretical line is not in complete agreement with the experimental points. In particular, in conditions in which the meniscus approaches most closely to the nip the theory is less satisfactory. Figure 5 shows that  $\lambda$  depends on the position of the meniscus and this result is in qualitative agreement with experiment, although as already explained the experiments were of only sufficient accuracy to enable a semi-quantitative comparison to be made. The dependence of  $\alpha$  on  $(T/\mu U)$  given by equation (2.31) is a result of great importance, which receives its confirmation in the theory of the critical conditions.

All these results have been obtained from a treatment that involves many approximations. It will be remembered that boundary conditions have only been satisfied at the meniscus, and even then only approximately and in a region close to the axis of symmetry. The fluid velocity at the surfaces of the rollers does not have the correct value. Nevertheless, in spite of these shortcomings, important results have been obtained which account for the main features



of the even flow régime, and are essential for the explanation of the transition to the ribbed flow pattern.

The explanation of the physical basis of the change in flow conditions given in §3.2 gives results which are qualitatively in complete agreement with the experiment. In this explanation the proportionality between  $\alpha$  and  $(T/\mu U)$  established by the theory of the even flow régime is of decisive importance. Without these results, the role played by the ratio  $(\mu UR/Th)$  cannot be explained. The quantitative prediction of critical conditions is obviously a much more exacting requirement but here again the theory is fairly successful. In this case it must be remembered that experimental difficulties in recognizing reliably the first appearance of uneven flow are considerable. There is no doubt that, with more elaborate methods of viewing the surfaces of the liquid sheets over the rollers, it would have been possible to detect uneven flow for a value of  $(\mu UR/Th)$  substantially lower than 62. A factor as large as 2 could possibly arise from this cause alone. Without any added refinements of viewing, it was always possible to observe uneven flow at speeds lower than those finally recorded in our experiments. In this region the unevenness was of such small amplitude that an observer could not consistently judge its true onset, but selected values of the speed varied by almost a factor of 2. A particular small amplitude was therefore adopted as a standard, the use of which made consistent results possible.

For this reason, the difference between  $\Theta^2$  from experiment (62) and from theory (28) is in the expected direction and is no doubt largely to be attributed to this experimental difficulty.

On the other hand it is likely that the theory is in error owing to several approximations. During the course of the numerical calculations it was obvious that comparatively small changes in certain terms could have a large effect on the value of the product  $(B)(C)$ . The expression for  $\partial p/\partial x$  near the meniscus is probably incorrect and the change in  $\lambda$  for the perturbed meniscus is derived from the variation of  $\lambda$  with position when conditions are in equilibrium. These may both be important sources of error.

With these facts in mind, it is perhaps unreasonable to expect closer numerical agreement. The successful explanation of all the qualitative experimental results and the approximate quantitative agreement between theory and experiment establishes the general adequacy of the treatment of the problem.

The authors would like to express their gratitude in particular to Mr A. Mariage, Mr E. W. H. Selwyn and Mr A. K. Soper of these laboratories, who, in preliminary discussion on this problem, helped to suggest possible physical explanations of the observed phenomena, one of which was developed to form the basis of the account in this paper. Their support has been most encouraging.

Next, the authors are indebted to Sir Geoffrey Taylor, who discussed the problem at length and made available unpublished work bearing on it. His criticism has been very helpful and stimulating.

Finally, Dr J. R. A. Pearson discussed his problem with us and kindly made available his publication while in draft form, for which we should like to express our acknowledgements.

This paper is Communication No. 2143 H from the Kodak Research Laboratories.

## REFERENCES

- BANKS, W. H. & MILL, C. C. 1954 *Proc. Roy. Soc. A*, **223**, 414.  
 HOPKINS, M. R. 1957 *Brit. J. Appl. Phys.* **8**, 442.  
 PEARSON, J. R. A. 1960 *J. Fluid Mech.* **7**, 481.

## Appendix

We require an approximate solution of equation (3.11). Let us introduce the variable  $\xi$  defined by equation (2.1) and put

$$G = H\sigma^{\frac{1}{2}}. \quad (\text{A. 1})$$

Then substitution in equation (3.11), together with the definition of  $\sigma$  from equation (2.4), gives

$$\frac{d^2H}{d\xi^2} = H \left[ 3 \left( \frac{1}{\sigma} - \frac{1}{2\sigma^2} \right) + N \right], \quad (\text{A. 2})$$

where  $N$  is defined in equation (3.15). An approximate solution of equation (A. 2) may be obtained by replacing the term in square brackets by its value at the nose of the meniscus. The result may then easily be improved by successive approximations.

We shall therefore consider

$$\frac{d^2H}{d\xi^2} = \rho^2 H, \quad (\text{A. 3})$$

where

$$\rho^2 = N + 3 \left( \frac{1}{\sigma_0} - \frac{1}{2\sigma_0^2} \right), \quad (\text{A. 4})$$

and measure  $\xi$  from the point where the meniscus cuts the axis of symmetry. The perturbation must vanish as the nip is approached, i.e. as  $\xi$  tends to  $-\infty$ , so the solution of equation (A. 3) may be written

$$H = B e^{\rho\xi}. \quad (\text{A. 5})$$

The condition in equation (3.14) gives the values of  $B$  immediately, and substitution in equation (3.18) results in the inequality

$$\frac{d\lambda}{d\xi} < \frac{\sigma_0^3}{3\sigma_1^2} \left[ 3 \left( \frac{\sigma_1}{\sigma_0} \right)^2 \left( 1 - \frac{\lambda}{\sigma_0} \right) - \left( \frac{\sigma_1 - 1}{2k} \right)^{\frac{1}{2}} \Theta^{-1} - \sigma_1^2 \Theta^{-2} N \right] \left[ \rho - \frac{3(\sigma_0 - 1)^{\frac{1}{2}}}{2^{\frac{1}{2}}\sigma_0} \right]. \quad (\text{A. 6})$$

Since by definition

$$\sigma_1 = (1 + \beta) \sigma_0, \quad (\text{A. 7})$$

then

$$\frac{d\lambda}{d\xi} = 2^{\frac{1}{2}}(1 + \beta) (\sigma_0 - 1)^{\frac{1}{2}} \frac{d\lambda}{d\sigma_1}, \quad (\text{A. 8})$$

and the condition for instability may be written

$$4 \cdot 24(1 + \beta)^4 \frac{(\sigma_0 - 1)^{\frac{1}{2}}}{\sigma_1} \frac{d\lambda}{d\sigma_1} < \left[ 3 \left( \frac{\sigma_1}{\sigma_0} \right)^2 \left( 1 - \frac{\lambda}{\sigma_0} \right) - \left( \frac{\sigma_1 - 1}{2k} \right)^{\frac{1}{2}} \Theta^{-1} - \sigma_1^2 \Theta^{-2} N \right] \left[ \rho - \frac{3(\sigma_0 - 1)^{\frac{1}{2}}}{2^{\frac{1}{2}}\sigma_0} \right]. \quad (\text{A. 9})$$

By developing the right-hand side of equation (A. 2) as a power series in  $\xi$  further approximations may readily be derived. We shall omit them here, since their effect on the expression (A. 6) is quite small, and moreover equation (A. 2) in any case is only valid in the immediate vicinity of the perturbed meniscus, so that extra terms are of very doubtful significance.